

Conversion of Oil Palm Empty Fruit Bunch (EFB) Biomass to Bio-Oil and Jet Bio-Fuel by Catalytic Fast-Pyrolysis Process

Halimatun Hamdan^{1*, 2}, Rozzeta Dolah¹, Haryanti Yahaya¹, Norsahika Mohd Basir² and Rohit Karnik³

¹Razak Faculty of Technology and Informatics, Universiti Teknologi Malaysia, Jalan Sultan Yahya Petra, 54100 Kuala Lumpur, Malaysia

²Zeolite and Nanostructured Materials Laboratory, Universiti Teknologi Malaysia, 81310 UTM Johor Bahru, Johor, Malaysia

³MIT Dept. of Mechanical Engineering, Massachusetts Institute of Technology, Cambridge, Massachusetts 02139, USA

Oil palm empty fruit bunch (EFB) biomass is a potential source of renewable energy. Catalytic fast-pyrolysis batch process was initially performed to convert oil palm EFB into bio-oil, followed by its refinement to jet bio-fuel. Crystalline zeolites A and Y; synthesised from rice husk ash (RHA), were applied as heterogeneous catalysts. The catalytic conversion of oil palm EFB to bio-oil was conducted at a temperature range of 320-400°C with zeolite A catalyst loadings of 0.6 - 3.0 wt%. The zeolite catalysts were characterised by XRD, FTIR and FESEM. The bio-oil and jet bio-fuel products were analysed using GC-MS and FTIR. The batch fast-pyrolysis reaction was optimised at 400°C with a catalyst loading of 1.0 wt%, produced 42.7 wt% yields of liquid bio-oil, 35.4 wt% char and 21.9 wt% gaseous products. Analysis by GCMS indicates the compound distribution of the liquid bio-oil are as follows: hydrocarbons (23%), phenols (61%), carboxylic acids (0.7%), ketones (2.7%), FAME (7.7%) and alcohols (0.8%). Further refinement of the liquid bio-oil by catalytic hydrocracking over zeolite Y produced jet bio-fuel, which contains 63% hydrocarbon compounds (C₈-C₁₈) and 16% of phenolic compounds.

Keywords: empty fruit bunch; bio-oil; zeolite; Catalytic Fast-Pyrolysis; jet bio-fuel

I. INTRODUCTION

Global primary energy consumption increases by 37% between 2013 and 2035. Fossil fuels remain the dominant form of energy in 2035 with a share of 81%, down from 86% in 2013. Generally, the decline in oil and coal consumption is offset by an increase demand in gas and renewables (Duncan, 2011; Khalid & Audrey, 2012). The development of renewable fuel resources has attracted considerable attention because of the global environmental concerns and the exhaustion of fossil fuels resources (Lucas *et al.*, 2010). A viable alternative way of solving these problems is the production of hydrocarbon from inexpensive biomass waste sources. The current share of biomass in the net final energy consumption by end-use sector is 14%; which comprises

heating and cooling at 12.6%, transportation at 0.8% and electricity at 0.4% (Kristin *et al.*, 2016). The increasing demand by the aviation industry for alternative fuels that offers potential environmental benefits, has accelerated advances in exploring new generation of renewable bio-fuels sources. Biomass, also known as lignocellulosic material represents a valid alternative source to initially produce liquid bio-oil and finally jet bio-fuel, without competing with food crops and promote reduction of carbon emission (Jozsef *et al.*, 2014). Bio-oil derived from the pyrolysis of biomass is considered to be a promising second-generation energy-laden fuel.

Palm oil production is on a steeply rising path because of the rapid expansion of the food and manufacturing industries. As one of the largest producers and exporters of

*Corresponding author's e-mail: halimatonhamdan@utm.my

palm oil, Malaysia has seen the potential of oil palm biomass, in the form of empty fruit bunch (EFB), as a renewable energy source. Malaysia's palm oil sector generates an estimated 100 million dry tonnes of biomass in 2020; 18 million tonnes is EFB. The vast majority of the oil palm biomass being generated today is returned to the field to release its nutrients and replenish the soil. However, there is also the potential to utilise the EFB biomass for a variety of additional end uses, with the highest-value opportunities being biofuels and bio-based chemicals.

There are three main components in oil palm EFB, namely cellulose, hemicellulose and lignin. These three components are insoluble in most chemical solvents due to crosslinking, which can be hardly degraded at low temperature. Liquefaction of palm oil EFB using thermochemical degradation process such as pyrolysis has been conducted at high temperature (400–600°C) in the absence of oxygen over a short period of time (George & Avelino, 2007).

To date, fast-pyrolysis is the most promising technology for biomass conversion. Fast-pyrolysis performs thermochemical decomposition of a lignocellulosic compound through rapid heating at a temperature range of 350°C to 800°C in the absence of oxygen; converting it to liquid bio-oil with gas and char as by-products (Anjani *et al.*, 2016; Anthony, 2012; Faisal *et al.*, 2011). It has been reported that up to 46 wt% yields of bio-oil, pyrolysed at 600°C has been generated (Wan *et al.*, 2012). Unfortunately, the characteristics of liquid bio-oil produced were physically dark brown in color, viscous and corrosive, relatively unstable with a complex structure that limits its potential for direct use in engines or turbines (Phuong *et al.*, 2013; Mandana *et al.*, 2014).

In the last few decades, numerous researches have been conducted, focused on using heterogeneous catalyst toward the enhanced and efficient conversion of biomass to bio-oil. Without catalysts, it is postulated that biomass pyrolysis would result in a high amount of phenol and very low yield of liquid bio-oil. Therefore, suitable heterogeneous catalysts have to be designed and introduced in the process in order to improve the conversion efficiency and capacity, preferably at a lower temperature range and enhance yield and quality of the bio-oil (Ravindra *et al.*, 2016; Kiky *et al.*, 2015; Wan *et al.*, 2012).

Hydrocarbons in the range of gasoline (jet fuel) can be obtained by refining or upgrading the bio-oil. It is also vital to upgrade further the bio-oil derived from biomass to a non-oxygenated liquid fuel that possesses desirable properties for combustion. The elimination of oxygen by deoxygenation and catalytic cracking are the two main approaches for upgrading liquid bio-oil to jet bio-fuel (Yinbin *et al.*, 2016; Yu *et al.*, 2017). However, to our knowledge, hydrocarbon products derived from bio-oil catalytic cracking are low carbon hydrocarbons; whereby they do not meet the standard specification requirement for jet fuels (ASTM D1655-2012, 1994) (Peiyan *et al.*, 2013). High oxygenated bio-oil content; due to the presence of reactive chemical components like phenols, carboxylic acids, aldehydes, ketones and alcohols, reduce the quality of bio-oil.

Consequently, the bio-oil has increased acidity, strong corrosiveness and reduced heating value; which hinder its direct use as fuel (Shouyun *et al.*, 2018). One effective method to improve bio-oil quality is to reduce the content of oxygenated compounds through catalytic reactions. Deoxygenation and the catalytic cracking reaction is an efficient method for bio-oil upgrading, in which it selectively removed oxygen from oxygenated compounds in bio-oil. Therefore, the second step of catalytic reaction needs to be designed in order to refine and upgrade the oil palm EFB bio-oil to jet bio-fuel.

Various heterogeneous catalysts have been investigated for conversion of bio-oil to jet bio-fuels; wherein the choices of catalysts are very important, especially during catalytic cracking and deoxygenation process. Zeolites are crystalline aluminosilicates with three-dimensional framework structures that form pores with uniform sizes of molecular dimensions (Theo, 2007; Saifuddin & Kumaran, 2015). Synthetic zeolites have been designed, synthesised and applied in many chemical reactions and processes; due to the framework nanostructure, ion-exchange abilities, chemical composition, pore size distribution and both acidic-basic characteristics (Nikolaos *et al.*, 2015; Maryam *et al.*, 2014; Javier *et al.*, 2012). Locally synthesised and modified zeolites is economical and environmentally friendly. Zeolite A may be efficiently applied in the petrochemical industry, as molecular sieves, adsorbent and

zeolite Y as a heterogeneous catalyst for cracking and hydrocracking of hydrocarbon molecules into oil and gas (Halimaton *et al.*, 1997; Halimaton & Yeoh, 1993). However, the pore size of zeolite Y needs further modification in order to improve the cracking efficiency of heavy hydrocarbon bio-oil to light jet range alkane.

The paper reports the catalytic conversion of oil palm EFB biomass into bio-oil over heterogeneous zeolite catalysts, to produce various organic oxygenated hydrocarbon compounds with a carbon chain range from C₄ to C₁₈. It demonstrates that fast pyrolysis of oil palm EFB, in the presence of locally synthesised zeolite catalysts, could efficiently convert EFB biomass into high yield liquid bio-oil at a low degradation temperature range of 320–400°C. The pyrolysed bio-oil was further refined by catalytic hydrocracking pyrolysis to form jet bio-fuels.

II. MATERIALS AND METHOD

A. Feedstock Materials

Oil palm EFB fibres; the feedstock material, was collected from a palm oil mill at Sg. Sumun, Bagan Datuk, Perak. The EFB fibres were pre-washed and sun-dried, followed by grinding into microfibers of about 100-150 µm in length. The EFB microfibers were weighed prior to the catalytic pyrolysis process.

B. Zeolite Catalysts

Zeolite catalysts applied throughout the course of the pyrolysis process were prepared in the laboratory following the procedure described by Hamdan (Halimaton *et al.*, 1997; Halimaton & Yeoh, 1993). The types of zeolites synthesised were chosen based on the desired catalytic properties and functions: Zeolite A contains the highest amount of exchangeable sodium cations needed for the pyrolysis of biomass and zeolite Y has high proton content which constitutes to strong Bronsted acidity of the catalyst; properties required by the cracking process for the refinement of bio-oil to jet bio-fuel.

1. Synthesis of Zeolite A

A silicate solution was prepared by mixing rice husk ash SiO₂ (10.65 g) into 150 mL NaOH solution with heating

and stirring. An aluminate solution was prepared by mixing NaAlO₃ (27.07 g) and NaOH solution with vigorous stirring. The silicate solution was mixed with the aluminate solution to form a reactant mixture, with the following composition: 8.7Na₂O:Al₂O₃:SiO₂:560H₂O (Halimaton & Yeoh, 1993). The mixture was then transferred into a 500 mL polyethylene bottle and placed in an oven at 100°C for 6 hours. The product was filtered and washed with distilled water. Finally, zeolite NaA was calcined in the furnace at 550°C for an hour.

2. Synthesis of Zeolite Y

An aluminate solution was prepared by mixing 19.56 g of sodium aluminate (NaAlO₂) and 50 mL NaOH solution in a Teflon beaker followed by vigorous stirring and heating. In the meantime, rice husk ash SiO₂ (47.97 g) was dissolved in 150 mL NaOH solution with heating and stirring. The alkaline aluminate solution and the aqueous silicate solution was mixed in a Teflon bottle, followed by stirring until a gel was formed with a mixture composition: 6.4Na₂O:1Al₂O₃:12SiO₂:180H₂O (Halimaton & Yeoh, 1993). The gel was kept in the Teflon bottle and left to age for at least 8 hours in the oven at 105°C. The solid product was filtered, repeatedly washed with distilled water and dried in the oven at 100 °C. The zeolite Y was calcined at 550°C for an hour.

3. Ion-exchange of zeolites

Ion-exchange in zeolites is the process in which the cations originally present within the intracrystalline pore system are replaced by other cations in order to either ensure complete removal of extraneous charge-balancing cations or introduce subsequent Bronsted acidity to the framework. In our study, Na⁺ cations present in the synthesised zeolite Y was ion-exchanged with NH₄⁺ cations. In a typical preparation, 1 g of zeolite Y was treated in a 50 ML of 1M NH₄NO₃ solution. The mixture was stirred for 2 hours at 60°C. The NH₄Y zeolite crystals were filtered, washed with distilled water and air-dried. The protonated zeolite Y (HY) was obtained by calcination of the NH₄Y at 500°C for 3 hours in a furnace.

C. Batch Catalytic Fast-pyrolysis of Oil Palm EFB to Bio-oil

Batch catalytic fast-pyrolysis process of oil palm EFB to bio-oil was conducted at the following temperature: 320°C, 350°C, 370°C and 400°C with EFB amount of 50 g and reaction time of 2 hours. The starting temperature is the temperature for zeolite activation. The weight of bio-oil and char collected for each batch was recorded.

The yield of the liquid bio-oil and conversion of the process was calculated and deduced from the following formula:

$$\text{EFB Conversion (\%)} = \frac{\text{EFB Feed (g)} - \text{Char (g)}}{\text{EFB Feed (g)}} \times 100 \quad (1)$$

$$\text{Bio-oil Yield (wt\%)} = \frac{\text{Liquid product (g)}}{\text{EFB Feed (g)}} \times 100 \quad (2)$$

Gases yield (wt%) =

$$\frac{\text{EFB Feed} - [\text{Liquid product (g)} + \text{Char (g)}]}{\text{EFB Feed (g)}} \times 100 \quad (3)$$

Zeolite Na-A (1 g) which was pre-activated at 320°C for 30 minutes, was mixed with 100 g EFB microfibrers and fed into the reactor. The reactor chamber was closed and secured in order to ensure an air-tight environment. It was flushed with N₂ gas for 15 minutes before it was slowly heated up to 320°C for 2 hours. The liquid bio-oil product was collected at the outlet valve. The same process was repeated at 350°C, 370°C and 400°C.

Effect of catalyst loading on the EFB pyrolysis at optimised temperature was studied. The reaction consists of an EFB amount of 50 g, the reaction time of 2 hours and the following zeolite A catalyst loadings: 0.3 g (0.6 wt%), 0.5 g (1 wt%), 1 g (2 wt%) and 1.5 g (3 wt%). The liquid products were analysed using gas chromatography-mass spectrometry (GC-MS) and FTIR.

The catalytic fast-pyrolysis process was performed using a 500 mL batch reactor system. The experimental setup for the process is shown in Figure 1.

D. Catalytic Cracking of Bio-oil to Jet Bio-fuel

The refinement of bio-oil to jet bio-fuel by the catalytic cracking process was done using a 500 mL batch reactor. 50 mL bio-oil was mixed with 50 mL acetonitrile (ACN); as the solvent, and stirred for 30 minutes. Zeolite HY (0.5 g), which was pre-activated at 400°C for 30 minutes, was added into the mixture and stirred for another 15 minutes. The solution was poured into the reaction chamber. At this point, the cracking reactor set up followed the same steps of the pyrolysis process. Thereafter, the reactor was then purged with flowing hydrogen for about 20 minutes to set the pressure and heated to 400°C for 4 hours. The resultant bio-fuel was collected at the outlet valve. The liquid products were analyzed using gas chromatography-mass spectrometry (GC-MS) and Fourier Transformed Infrared Spectroscopy (FTIR).

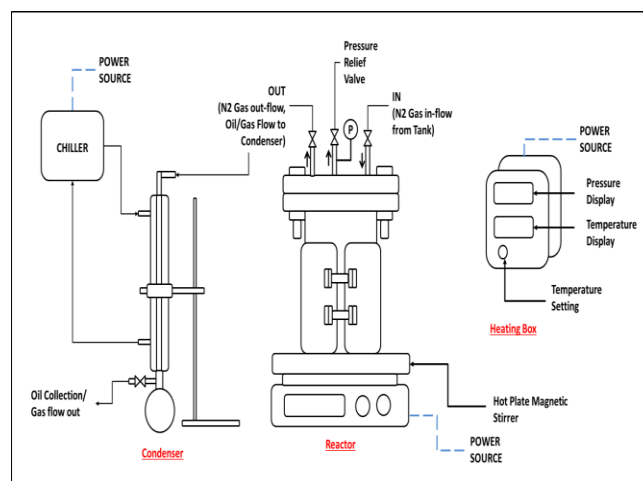


Figure 1. Experimental Set-up for Batch Fast-Pyrolysis Process

E. Characterization of Zeolites and Bio-oil

1. X-Ray Diffraction (XRD)

Powder X-ray Diffraction (XRD) is a means of qualitative and quantitative identification and characterisation of microcrystalline solids such as zeolites. It provides information on the long-range order, phase purity and changes in lattice parameters with changing composition.

XRD analysis was performed on Bruker Advance D8 using Siemens 5000 diffractometer with CuK_α radiation, operated at 40 kV and 20 mA ($\lambda = 1.5418 \text{ \AA}$). Samples were scanned in the range of $2\theta = 5 - 50^\circ$. A step interval of $0.05^\circ 2\theta$ with

a count time of 1 s per step was used. Reflection positions and d-spacings were determined from the raw data using the automated data analysis programs. Powder sample (1.0 g) was ground to a fine powder and pressed between two glass slides before mounting on a sample holder.

2. Fourier Transformed Infrared Spectroscopy (FTIR)

Fourier Transformed Infrared (FTIR) spectroscopy is a method of structure characterisation giving information on short-range and long-range bond order caused by lattice coupling, electrostatic and other effects. FTIR spectra enable assignments of infrared frequencies to structural properties or characteristics of microcrystalline zeolites.

Samples were characterised by Perkin Elmer Spectrum One FTIR spectrometer using the KBr pellet method. Samples were finely pulverised with dry KBr with a ratio of 1:100 and palletised to a thin wafer under 10 tonnes pressure. IR spectra were recorded at 25°C in the wavenumber range of 400-4000 cm^{-1} .

3. Field Emission Scanning Electron Microscopy (FESEM)

Morphology of samples was examined using JEOL JSM-670F field emission scanning electron microscope operating at 15 kV. FESEM images provide information about crystal size, structural defects within the crystal and three-dimensional visualisation of sample surfaces. Since the surface of zeolites get easily charged when subjected to the electron beam, before analysis, all the synthesised zeolites were coated with platinum or carbon film using a SEM auto fine-coater unit model JEC-3000FC or EC-32010CC respectively.

4. Gas Chromatography-Mass Spectrometry (GCMS)

To evaluate catalytic reaction products, Gas Chromatography-Mass Spectrometry (GC-MS) analysis technique was applied. The liquid products were also analysed using Fourier Transformed Infrared Spectroscopy (FTIR) in order to detect and identify the functional groups present in the bio-fuel and jet bio-fuel products. The settings for all methods and analysis are as follows:

The liquid products from the catalytic pyrolysis process were characterised using Agilent GC-MS instrument

(5973/6890N) equipped with BP5MS-column (29.6 m x 0.25 mm x 0.25 μm ID). A sample amount of 0.5 μL was injected for each analysis. The sample was analysed by the splitless method with helium (He) as the carrier gas. Analysis temperature was increased from 60°C to 300°C at the rate of 15 °C/min. At 210°C, the process was held for 2 minutes. The product yield of liquid bio-fuel from the catalytic pyrolysis was manually calculated based on area percentage.

III. RESULT AND DISCUSSION

A. Physicochemical Properties of Zeolite A and Zeolite Y

The X-ray diffractograms of zeolite A and zeolite Y are shown in Figure 2. The zeolites synthesised were identified by direct comparison and peaks matching with the standard simulated diffraction patterns of Linde Type-A (LTA) and faujasitic (zeolite Y) zeolites (Micheal & John, 2007). The XRD pattern of synthesised zeolite A displays the characteristic reflections of crystalline zeolites NaA and confirms the absence of impurity or amorphous phase domain in the sample.

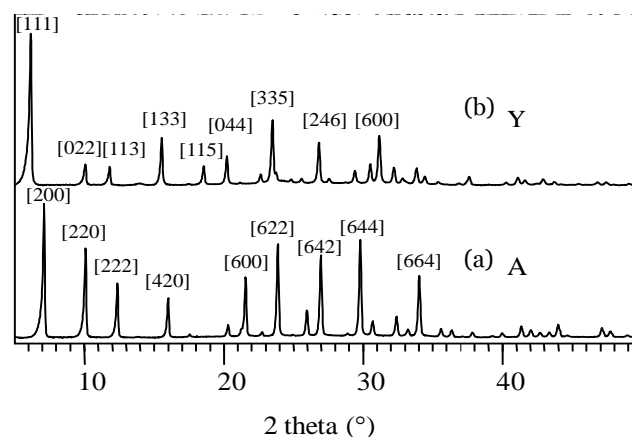


Figure 2. X-Ray Diffractogram for synthesised (a) Zeolite A and (b) Zeolite Y

Table 1. Peak List for Synthesized Zeolite A and Y (matched with Reference from Collection of Simulated XRD pattern by Treacy and Higgins J.B (Micheal & John, 2007))

Peak List for Zeolite A				
Pos. [°2θ]	Height [cts]	FWHM Left [°2θ]	d-spacing [Å]	Rel. Int. [%]
[111]				
[022]				
[113]				
[133]				
[044]				
[115]				
[335]				
[246]				
[600]				
[200]				
[220]				
[222]				
[420]				
[600]				
[622]				
[642]				
[644]				
[664]				

7.108	19605.65	0.1279	12.43661	100
10.0835	14357.25	0.1279	8.77243	73.23
23.8848	16992.13	0.1279	3.72563	86.67
27.0071	15875.8	0.1535	3.30158	80.98
29.825	19223.41	0.1791	2.99575	98.05
34.0514	11890.92	0.1791	2.63298	60.65

Peak List for Zeolite Y

Pos. [2θ]	Height [cts]	FWHM Left [2θ]	d-spacing [Å]	Rel. Int. [%]
6.1822	53207.78	0.1279	14.29672	100
10.103	11701.73	0.1279	8.75559	21.99
15.5939	19087.47	0.1279	5.68276	35.87
23.5474	22133.04	0.1279	3.77824	41.6

The peak positions of the observed pattern match the six most intense reflections of zeolite A at 2θ values of $7.12^\circ(200)$, $10.10^\circ(220)$, $23.90^\circ(622)$, $27.03^\circ(642)$, $29.85^\circ(644)$ and $34.08^\circ(664)$. Similarly, XRD pattern of the zeolite Y matches the reference peaks of faujasitic zeolite Y. The main XRD reflections at 2θ values tabulated in Table 1 are matched to the crystal planes of the faujasite structure: $6.17^\circ(111)$, $15.56^\circ(133)$, $23.49^\circ(335)$ and $27.58^\circ(246)$, which indicate that crystalline zeolite Y was formed.

The FTIR spectra of zeolite A and Y are presented in Figure 3. The details of the infrared transmission bands for both zeolites are shown in Table 2. The band at 1650 cm^{-1} is attributed to the O-H bending band, related to vibrations of adsorbed water in zeolite structures. The bands at 1007 and 768 cm^{-1} represent the asymmetric and symmetric stretching vibrations corresponding to the inner TO_4 tetrahedral structure (T=Si and Al), respectively. Moreover, the band at 553 and 570 cm^{-1} is assigned to the double ring external linkage indicating the existence of zeolite A and zeolite Y framework respectfully.

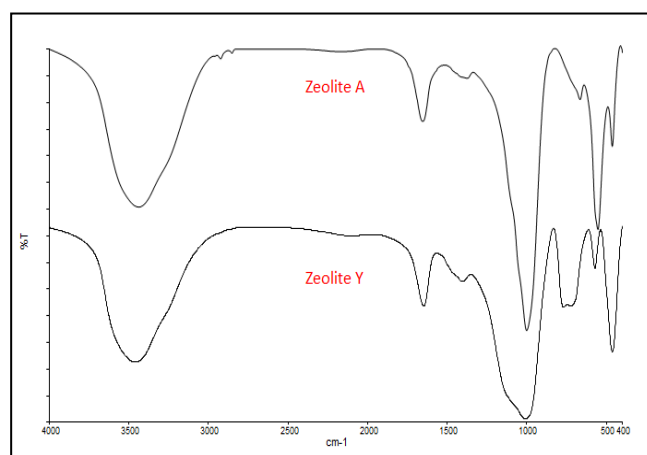


Figure 3. FTIR Spectra for Zeolite A and Y

Table 2. Infrared Transmission bands for Zeolite A and Y

Vibration mode	Zeolite A (cm^{-1})	Zeolite Y (cm^{-1})
O-H stretching	3436.89 (s)	3461.17 (s)
O-H bending	1651.67 (ms)	1645.45 (ms)
Asymmetric	1001.40 (s)	1007.22 (s)
Symmetric	666.07 (ms)	768.26 (ms)
Double ring	553.66 (m)	570.9 (m)
T-O bends (where T = Si or Al)	463.64 (ms)	460.85 (ms)

s=strong, ms= medium strong

FESEM images of both zeolite A and Y are shown in Figure 4(a) and 4(b), respectively. Figure 4(a) shows that the morphology of the sample is a single phase clusters of cubic crystalline structures, characteristic of zeolite A. The FESEM image of zeolite A depicts clusters of uniform cubic crystallites with well-defined edges and average particle size of $300\text{--}800\text{ nm}$ and no apparent agglomeration of particles. In contrast, it is observed that zeolite Y cubic crystals are less defined, irregular in shape and smaller in size (Figure 4(b)). They appear as large agglomerates of fused nanosized cubic crystallites, with an average size of 300 nm . Some amorphous silica particles of 10 to 50 nm in diameter are observed on the surface of zeolite Y.

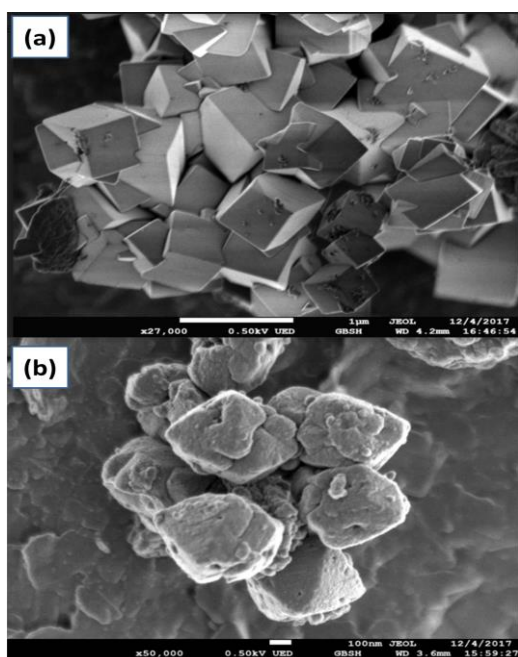


Figure 4. FESEM images of (a) Zeolite A. Scale bars of 100 nm with x27,000 magnification (b) Zeolite Y. Scale bars of 100 nm with x50,000 magnification.

B. Catalytic Fast-pyrolysis of Oil Palm EFB to Bio-oil

The pyrolysis reaction converted oil palm EFB to three main products: liquid bio-oil, solid carbonaceous residue (char) and non-condensable gas. Results in Table 3 demonstrate that the yield of liquid bio-oil, char and gas is 42.7 wt%, 35.4 wt% and 21.9 wt%, respectively.

Table 3. Product Yield of bio-oil composition converted from EFB over zeolite A catalyst by batch fast pyrolysis

Sample	Product yield (wt%)		
	Liquid	Char	Gaseous
Bio-oil	42.7	35.4	21.9

0.5 g Catalyst; 50 g EFB; 2 h and 400°C

Effect of temperature on the yield of bio-oil (wt%) is presented in Figure 5. The results show that the yield of liquid bio-oil increases proportionally with an increase in temperature. The same trend has been observed and reported by others (Mohamad *et al.*, 2016).

It is observed that the process was reaching optimisation at the temperature range of 370°C-400°C, followed by a decrease in the percentage of gas and char. It suggests that secondary cracking occurred at the temperature range, resulting in increased conversion of gases into bio-oil. The

reaction appeared to slow down significantly beyond 400°C as indicated by the lowest increase in bio-oil yield (0.6 wt%); presumably due to further decomposition of intermediate compounds into gaseous product and condensation of light volatile compounds into a liquid product at a higher temperature. The decrease in the yield of liquid bio-oil at a higher temperature beyond 400°C may be attributed to enhanced secondary cracking of the lighter hydrocarbon compounds into gaseous products such as methane, hydrogen, carbon monoxide and carbon dioxide. Consequently, the yield of char is inversely proportional to the increase in temperature; attributed to the efficient decomposition of vapours via secondary cracking which happened over the catalyst inside the reactor during the process (Bachrun & Arif, 2018). Therefore, the pyrolysis of oil palm EFB is optimised at 400°C; 58% conversion of EFB yields 39 wt% liquid bio-oil and 19 wt% gaseous products.

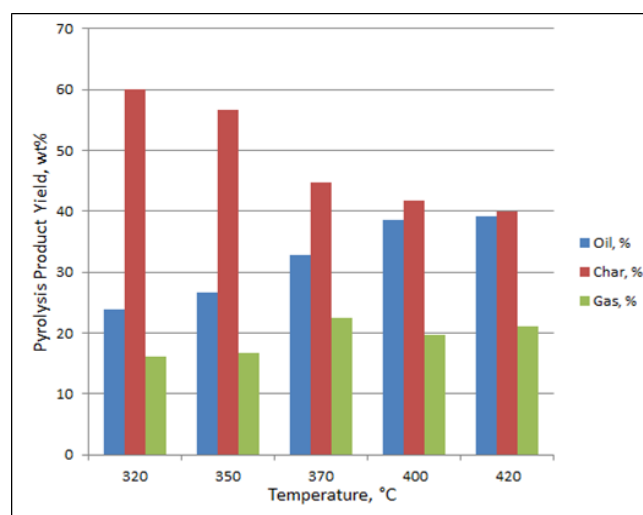


Figure 5. Effect of temperature on pyrolysis process product yield, (1 wt% of zeolite A catalyst, 100 g EFB, pyrolysis for 2 hours)

The influence of catalyst loading on the pyrolysis process of palm oil EFB is presented in Figure 6. The effect of catalyst loading (0.3 g, 0.5 g, 1.0 g and 1.5 g) was studied using zeolite A catalyst at 400 °C for 2 hours with 50 g of oil palm EFB. The data indicates that the yield of liquid bio-oil increased from 36 wt% to 39 wt% when the amount of catalyst increased from 0.3 g to 0.5 g, respectively. The increase in the liquid bio-oil product yield may be due to the proportional increase in the number of active sites of the zeolite A catalyst in the reaction. However, the yield of liquid

bio-oil decreased with a further increase of catalyst loadings; due to diffusion limitations when the catalyst is used in a high amount.

Overall, the data indicates that a catalyst loading of 0.5 g gives the highest yield of bio-oil (39 wt%) and the lowest yield of gas products (19 wt%). Therefore, the optimum catalyst loading for the process is 1 wt%.

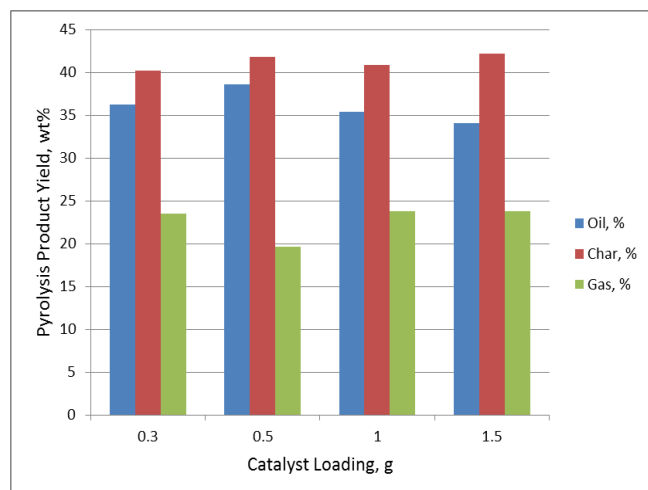


Figure 6. Effect of catalyst loading on pyrolysis product yield (zeolite A catalyst, 50g EFB, 400°C, 2 hours)

1. Chemical analysis of bio-oil by GCMS

In the fast pyrolysis process, oil palm EFB biomass was heated to 400°C without oxygen in order to produce a high yield of liquid bio-oil, together with solid char and gaseous byproducts. Bio-oil is a complicated mixture of various chemicals compounds; derived from the thermochemical degradation of biomass pyrolysis. The chemical compound distributions of liquid bio-oil were analysed using GCMS based on chemical functional groups. The distribution of compounds was semi-quantitatively determined by the percentage area of the chromatography peaks.

The analysis by GCMS on the compound distributions of liquid bio-oil is represented as green bands in Figure 7. The distributions of chemical compounds were determined by the percentage area of the chromatography peaks. In general, the composition of bio-oil products can be classified into nine main compounds which are hydrocarbon (C₈-C₁₅) and C₁₆-C₃₀), phenolic, ketone, alcohol, esters, acids (carboxylic acids), FAME (Fatty Acid Methyl Esters), methoxy benzene and nitrogenated compounds.

The GCMS analysis shows that the content of hydrocarbons in liquid bio-oil is 23%. The data recorded in our study are generally higher than those observed in previous studies (Shouyun *et al.*, 2018). The liquid bio-oil also contain phenols (61%), carboxylic acids (0.7%), ketones (2.7%), FAME (7.7%) and alcohols (0.8%). These chemical compounds were derived from the decomposition of cellulose, hemicellulose and lignin identified in the oil palm EFB biomass.

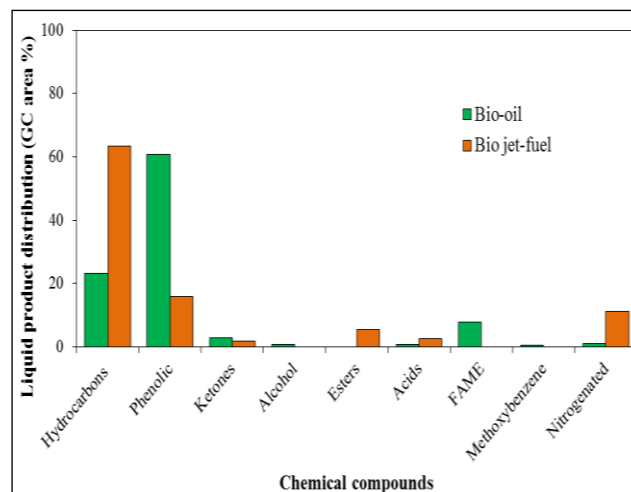


Figure 7. Liquid Product Distribution in bio-oil and jet bio-fuel products

C. Catalytic Cracking of Bio-oil to Jet Bio-fuel and Chemical Analysis by GCMS

Bio-oil obtained from EFB was further refined by catalytic cracking over zeolite HY catalyst in order to meet the specification of jet bio-fuel. Typically, commercial jet fuel consists of three main components, including alkanes, cyclic alkanes and aromatic hydrocarbons (ASTM D1655-2012, 1994). The deoxygenation and catalytic cracking reaction are required to produce jet fuel range hydrocarbons from oil palm EFB biomass.

The GCMS analysis on the compound distributions of refined bio-oil (jet bio-fuel) is represented by brown bands shown in Figure 7. The percentage composition of liquid bio-oil and jet bio-fuel shows a significant difference, where a higher percentage of hydrocarbon compounds (64%) is present in jet bio-fuel compared to bio-oil (23%). The jet bio-fuel over zeolite Y catalyst consists of a high selectivity to straight-chain alkane (36%) and aromatic hydrocarbons (28%). After the catalytic cracking process, the percentage of

phenolic compounds of 61% in bio-oil is tremendously reduced to 16% in the jet bio-fuel. This indicates that catalytic cracking and deoxygenation (hydrodeoxygenation, decarbonylation and decarboxylation) reactions have successfully transformed the oxygenated compounds detected in the bio-oil to hydrocarbon, which resulted in reduced oxygen content of the jet bio-fuel (Shouyun *et al.*, 2018). The high acidity content (Brønsted and Lewis acid sites) of the zeolite Y catalyst has effectively promoted the formation of hydrocarbon compounds through multiple chemical reactions. Apparently, reduced content of phenols in jet bio-fuel is the results from its transformation into hydrocarbons through hydrogenation reactions over zeolite Y catalyst.

The percentage distribution of ketones; which are responsible for the low heating value of bio-oil was also decreased after refinement reaction. This is due to the transformation of ketones to alcohols through the reduction of C=O bonds in hydrogenation reactions (Wu Jun, 2012). The alcohols formed were then transformed to hydrocarbons or esters during the catalytic process. The FAME content in jet bio-fuel is not detected. This suggests that FAME has been completely converted into relatively stable esters through catalytic cracking and deoxygenation reactions, which led to the increase of ester content (5.40%) in the jet bio-fuel. The decrease in acids, alcohols and ketones content is beneficial for further upgrading of the jet bio-fuel in terms of reducing corrosion for storage tanks and pipeline materials. This work demonstrated that the bio-jet fuel derived from bio-oil EFB was able to be converted into jet and diesel fuel range hydrocarbons by secondary catalytic reactions. The FTIR spectra of bio-oil and jet bio-fuel are shown in Figure 8.

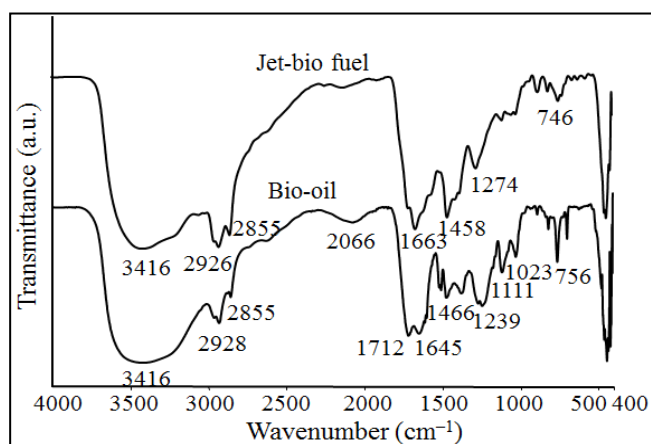


Figure 8. FTIR spectra for bio-oil and jet bio-oil

The broad band in both spectra at 3200-3500 cm^{-1} is assigned to the absorption of hydroxyl group attributed to phenolic and alcoholic compounds. Nevertheless, the intensity of the O-H stretching vibrations at 3400 cm^{-1} for the bio-jet fuel sample is reduced, indicating the occurrence of the deoxygenation process. This is in agreement with the results from GCMS whereby in the jet bio-fuel, a significant decrease amount of phenolic compounds was observed. The vibration at 2926 cm^{-1} and 2855 cm^{-1} (C-H stretching) of the samples indicates alkanes and alkenes' existence respectively. In addition, the presence of stretching vibrations of the carbonyl group (C=O) at 1645 cm^{-1} and 1712 cm^{-1} are attributed to the presence of ketone, aldehyde, ester and carboxylic group. On the other hand, the absence of absorption band at 1712 cm^{-1} in bio-jet fuel suggests that minimal amount of C=O compounds is present in the sample. GCMS and FTIR result indicates that a large amount of ketone, aldehyde, ester, carboxylic and phenol group is successfully converted to hydrocarbon compounds in the presence of zeolite HY catalyst.

IV. CONCLUSION

In summary, the conversion of oil palm EFB into bio-oil through catalytic fast pyrolysis process and the upgrading of bio-oil to jet bio-fuel via catalytic cracking process were successfully done. With heterogeneous catalysts like zeolite A and Y, a process of direct conversion of different phases of materials is easily achieved. In this study, the process temperature has been optimized at 400°C and of 1% catalyst loading ratio to EFB, giving a maximum yield of 39% bio-oil. The selectivity for phenol derivatives was 61%, while the

selectivity for liquid hydrocarbons was 23%. High phenolic content of the bio-oil is reduced by catalytic cracking process that successfully convert phenols into hydrocarbon compounds that leads to easier upgrading into jet bio-oil content. Oxygenated compounds in bio-oil was converted to jet fuel range hydrocarbons by deoxygenation (decarboxylation, decarbonylation and hydrodeoxygenation) and catalytic cracking reaction. The refinement process produced jet bio-fuel with the highest hydrocarbons content of 61% and phenol compounds of 16%. The study

demonstrates that catalytic transformation of bio-oil derived from oil palm EFB to jet bio-fuel is a viable method for developing green aviation biofuels from lignocelluloses biomass.

V. ACKNOWLEDGEMENT

The authors are indebted to UTM and Ministry of Higher Education for the NanoMITE-LRGS grant Vot 4L823.

VI. REFERENCES

- Abnisa, F, Daud, WW, Husin, WNW & Sahu, JN 2011, 'Utilisation possibilities of palm shell as a source of biomass energy in Malaysia by producing bio-oil in pyrolysis process', *Biomass and Bioenergy*, vol. 30, no. 5, pp. 1863-1872.
- Akia, M, Yazdani, F, Motaee, E, Han, D & Arandiyani, H 2014, 'A review on conversion of biomass to biofuel by nanocatalysts', *Biofuel Research Journal*, vol. 1, no. 1, pp. 16-25.
- Bi, P, Yuan, Y, Fan, M, Jiang, P, Zhai, Q & Li, Q 2013, 'Production of aromatics through current-enhanced catalytic conversion of bio-oil tar', *Bioresource Technology*, vol. 136, pp.222-229.
- Bridgwater, AV 2012, 'Review of fast pyrolysis of biomass and product upgrading', *Biomass and Bioenergy*, vol. 38, pp. 68-94.
- Cheng, S, Wei, L, Alsowij, MR, Corbin, F, Julson, J, Boakye, E & Raynie, D 2018, 'In situ hydrodeoxygenation upgrading of pine sawdust bio-oil to hydrocarbon biofuel using Pd/C catalyst', *Journal of the Energy Institute*, vol. 91, no. 2, pp. 163-171.
- Dang, PT, Le, HG, Pham, GT, Vu, HT, Nguyen, KT, Dao, CD, Le, GH, Hoang, TT, Tran, HT, Nguyen, QK & Vu, TA 2013, 'Catalytic pyrolysis of biomass by novel nanostructured catalysts. In micro/nano materials, devices, and systems', *International Society for Optics and Photonics*, vol. 8923, pp. 89234J.
- Diamantopoulos, N, Panagiotaras, D & Nikolopoulos, D 2015, 'Comprehensive review on the biodiesel production using solid acid heterogeneous catalysts', *Journal of Thermodynamics & Catalysis*, vol. 6, no. 1, p. 1.
- García-Martínez, J, Johnson, M, Valla, J, Li, K & Ying, JY 2012, 'Mesoporous zeolite Y—high hydrothermal stability and superior FCC catalytic performance', *Catalysis Science & Technology*, vol. 2, no. 5, pp. 987-994.
- Gollakota, AR, Reddy, M, Subramanyam, MD & Kishore, N 2016, 'A review on the upgradation techniques of pyrolysis oil', *Renewable and Sustainable Energy Reviews*, vol. 58, pp. 1543-1568.
- Graham-Rowe, D 2011, 'Agriculture: beyond food versus fuel', *Nature*, vol. 474, no. 7352, pp. S6-S8.
- Hamdan, H & Keat, YA 1993, 'Synthesis of zeolite Y from rice husks', *Malaysian Patent*, vol. 450, no. 1, pp. 4-22.
- Hamdan, H, Muhid, MNM, Endud, S, Listiorini, E & Ramli, Z 1997 '29Si MAS NMR, XRD and FESEM studies of rice husk silica for the synthesis of zeolites', *Journal of Non-Crystalline Solids*, vol. 211, no. 1-2, pp. 126-131.
- Hassani, M, Najafpour, G.D, Mohammadi, M & Rabiee, M 2014, 'Preparation, characterisation and application of zeolite-based catalyst for production of biodiesel from waste cooking oil', *J. Sci. Ind. Res. (India)*, vol. 73, no. 2, pp- 129-133.
- Huang, Y, Wei, L, Zhao, X, Cheng, S, Julson, J, Cao, Y & Gu, Z 2016, 'Upgrading pine sawdust pyrolysis oil to green biofuels by HDO over zinc-assisted Pd/C catalyst', *Energy Conversion and Management*, vol. 115, pp. 8-16.
- Huber, GW & Corma, A 2007, 'Synergies between bio-and oil refineries for the production of fuels from biomass', *Angewandte Chemie International Edition*, vol. 46, no. 38, pp. 7184-7201.
- Isahak, WNRW, Hisham, MW, Yarmo, MA & Hin, TYY 2012, 'A review on bio-oil production from biomass by

- using pyrolysis method', *Renewable and Sustainable Energy Reviews*, vol. 16, no. 8, pp. 5910-5923.
- Li, Y, Zhang, C, Liu, Y, Tang, S, Chen, G, Zhang, R & Tang, X 2017, 'Coke formation on the surface of 'Ni/HZSM-5 and Ni-Cu/HZSM-5 catalysts during bio-oil hydrodeoxygenation', *Fuel*, vol. 189, pp. 23-31.
- Liu, WJ, Zhang, XS, Qv, YC, Jiang, H & Yu, HQ 2012, 'Bio-oil upgrading at ambient pressure and temperature using zero valent metals', *Green Chemistry*, vol. 14, no. 8, pp. 2226-2233.
- Maesen, T 2007, 'The zeolite scene—anoverview', *Introduction to Zeolite Molecular Sieves*, vol. 38, p. 1.
- Pogaku, R, Hardinge, BS, Vuthaluru, H & Amir, HA 2016, 'Production of bio-oil from oil palm empty fruit bunch by catalytic fast pyrolysis: a review', *Biofuels*, vol. 7, no. 6, pp. 647-660.
- Popp, J, Lakner, Z, Harangi-Rakos, M & Fari, M 2014, 'The effect of bioenergy expansion: food, energy, and environment', *Renewable and Sustainable Energy Reviews*, vol. 32, pp. 559-578.
- Rahim, KA & Liwan, A 2012, 'Oil and gas trends and implications in Malaysia', *Energy Policy*, vol. 50, pp. 262-271.
- Rye, L, Blakey, S & Wilson, CW 2010, 'Sustainability of supply or the planet: a review of potential drop-in alternative aviation fuels', *Energy & Environmental Science*, vol. 3, no. 1, pp. 17-27.
- Saifuddin, N, Samiuddin, A & Kumaran, P 2015, 'A review on processing technology for biodiesel production', *Trends in Applied Sciences Research*, vol. 10, no. 1, p. 1.
- Sawin, JL, Sverrisson, F, Seyboth, K, Adib, R, Murdock, HE, Lins, C, Brown, A, Di Domenico, SE, Kielmanowicz, D, Williamson, LE & Jawahar, R 2016, *Renewables 2016 Global Status Report. Key findings. A Record Breaking Year for Renewable Energy: New Installations, Policy Targets, Investment and Jobs. Mainstreaming renewables: guidance for policy makers.*
- Sembing, KC, Rinaldi, N & Simanungkalit, SP 2015, 'Bio-oil from fast pyrolysis of empty fruit bunch at various temperature', *Energy Procedia*, vol. 65, pp. 162-169.
- Sukiran, MA, Loh, SK & Bakar, NA 2016, 'Production of bio-oil from fast pyrolysis of oil palm biomass using fluidised bed reactor', *J. Energy Technol. Policy*, vol. 6, pp. 52-62.
- Sutrisno, B & Hidayat, A 2018, 'Pyrolysis of palm empty fruit bunch: yields and analysis of bio-oil', In *MATEC Web of Conferences*, EDP Sciences, vol. 154, p. 01036.
- Treacy, MM & Higgins, JB 2007, *Collection of simulated XRD powder patterns for zeolites fifth (5th) revised edition.* Elsevier.